

**OPTIMIZATION OF THE SUBSTRATE PREHEAT TEMPERATURE FOR  
THE ENCAPSULATION OF FLIP CHIP DEVICES**

**By**

**C-Y. Huang, Ph.D.<sup>1</sup>, K. Srihari, Ph.D.<sup>1</sup>, and P. Børgesen, Ph.D.<sup>2</sup>**

**<sup>1</sup>Department of Systems Science and Industrial Engineering  
State University of New York  
Binghamton, New York 13902-6000.**

**<sup>2</sup>Universal Instruments Corporation  
Binghamton, New York 13902-0825.**

# OPTIMIZATION OF THE SUBSTRATE PREHEAT TEMPERATURE FOR THE ENCAPSULATION OF FLIP CHIP DEVICES

## ABSTRACT

Flip Chip On Board (FCOB) technology involves the bonding of bare die directly onto a Printed Circuit Board (PCB). The interconnections are provided by solder bumps which are arranged in the area under the chip. Encapsulation is the preferred strategy used to reduce the impact of the thermal stress that results from the mismatch in the Coefficient of Thermal Expansion (CTE) between the silicon chip and the substrate. The length of time needed for the dispensing and capillary flow of the encapsulant is one of the important factors that inhibits the high volume use of FCOB technology. Pre-heating the substrate prior to and during the dispensing of the encapsulant enhances its flow characteristics by reducing its viscosity.

This research addressed the feasibility of using a substrate preheat temperature which is higher than the manufacturer's recommendation in order to reduce the cycle time of the encapsulation process while concurrently ensuring package reliability. Defects that may be caused by increasing the substrate preheat temperature were discussed and evaluated. A statistical model was generated to help determine the optimal substrate preheat temperature for given chip dimensions, standoff height, surface texture, etc. Using the substrate preheat temperature determined by the model, the flow time of the encapsulant could be reduced by more than a factor of two while concurrently ensuring a 6 $\sigma$  quality level.

**Keywords:** Printed Circuit Board Assembly, Direct Chip Attach, Flip Chip on Board, Encapsulation, Underfill.

# **OPTIMIZATION OF THE SUBSTRATE PREHEAT TEMPERATURE FOR THE ENCAPSULATION OF FLIP CHIP DEVICES**

## **1.0 INTRODUCTION**

Flip Chip On Board (FCOB) technology provides a path for the electronics packaging industry to accommodate the need for greater product functionality while concurrently minimizing space and weight.

This approach involves bonding bare die directly to the Printed Circuit Board (PCB). The interconnections are provided by the solder bumps which are arranged in the area under the chip [1]. The mismatch in the Coefficient of Thermal Expansion (CTE) between the silicon chip and the substrate is a critical factor in FCOB technology. Encapsulation is the preferred strategy used to reduce the impact of the thermal stress that results from this CTE mismatch [2].

The long dispensing and curing cycle of the underfill material inhibits the high volume use of the FCOB technology [3]. A typical encapsulant dispensing cycle depends on the capillary flow of the underfill material. Significant effort has been (and is being) expended by manufacturers of underfill materials to enhance the flow characteristics of their materials by improving the surface tension and the wetting characteristics of encapsulants, reducing their viscosity, optimizing particle shapes, etc. Pre-heating of the substrate prior to the dispensing of the underfill material also enhances an encapsulant's flow characteristics [2]. The substrate should remain at the elevated temperature during the underfill process. This improves the flow characteristics of the underfill material by reducing its viscosity.

The substrate preheat temperature recommended by different manufacturers varies slightly. The typical temperature range is between 70°C and 80°C. Indications are that this temperature range could be acceptable, but sub-optimal. The present research addresses the feasibility of using a higher (optimal) substrate preheat temperature to reduce the process cycle time while concurrently ensuring package reliability. Defects that may be caused by increasing the substrate preheat temperature are discussed and evaluated. While underfill materials flow faster at a higher substrate preheat temperature, gelling could begin earlier. Clearly, the encapsulant flow needs to be completed before gelling commences. Model experiments were done using test coupons to provide an understanding of the flow behavior. The difference between the specimens used in the model experiments and an actual assembly was then characterized, and the results were corrected to correspond to the actual assembly scenario. The corrections included surface texture effects, differences in wetting, etc. The encapsulant studied in this research is widely used in industry. Its manufacturer recommended preheat temperature is 70°C. A statistically valid model was generated to help determine the optimal substrate preheat temperature given information on factors such as the chip dimensions, the standoff height, the surface texture, etc. The model can be generalized to other candidate materials as well as other applications. The reduction in the process cycle obtained by using the predicted optimal substrate preheat temperature was also assessed.

## **2.0 CONCERNS IMPOSED BY THE USE OF HIGH SUBSTRATE PREHEAT TEMPERATURES**

Some of the potential consequences of using a high substrate preheat temperature during the encapsulation of an FCOB device are given below [3].

- ❑ Defects such as filler settling and the formation of voids in the underfill could subsequently affect the package's fatigue life.
- ❑ Other effects which can not be detected by cross sectioning or acoustic microscopy may also influence the reliability. Examples include insufficient encapsulant/chip or encapsulant/substrate interface adhesion. Flux residues were found to melt at a temperature of around 50°C. Therefore, the presence of any flux residue related defect may be influenced by the substrate preheat temperature used. Possible defects include the effect on material adhesion characteristics, cure kinetics, and the properties of the cured material.
- ❑ The increase in preheat temperature results in a decrease in encapsulant viscosity. However, the enhanced temperature also accelerates chemical reactions resulting in faster gelling. The flow of the underfill needs to be completed before gelling occurs.

## **2.1 Evaluation of Possible High Preheat Temperature Induced Defects**

Fresh encapsulant material, which was stored for less than five hours at room temperature, was flowed in between two glass slides with a 0.076 mm (3 mil) standoff height. The encapsulant material was dispensed onto glass slides which were heated to 70°C and 100°C in two experiments, respectively. Specimens were removed from the hot plate when the encapsulant flowed to a distance of 12.7 mm (0.5 inches). When a substrate preheat temperature of 70°C was used, the specimen was kept on the hot plate for around three minutes while the specimen was kept on the hot plate for one minute when a substrate preheat temperature of 100°C was used. Both these specimens were left at room temperature for five minutes and then cured for two hours at 150°C. The specimens generated using the manufacturer's suggested substrate preheat

temperature (70°C) were compared with the one generated using a 100°C substrate preheat temperature.

A sample size of two was used to ensure the validity of the results.

The specimen that was underfilled using a preheat temperature of 100°C exhibited voids with a diameter of approximately 0.0127 mm (0.5 mils). Voids were found to be more frequent near the top glass slides.

Air bubbles were seen in the syringe prior to dispensing and a similar scenario was observed for the sample generated using the manufacturer's suggested preheat temperature (70°C). The preheat temperature did not increase the amount or the size of the voids. While this encapsulant was highly filled, filler settling was not observed at either substrate preheat temperature (70°C and 100°C). No other significant defect was seen at the higher substrate preheat temperature (100°C). Other possible consequences, such as the impact on interface adhesion, will be explored in the near future (in related research efforts).

## **2.2 Flow Experiments to Ensure That Flow Is Completed Before Gelling Occurs**

The influence of different factors on the completion of encapsulant flow before the onset of gelling is application specific. The factors that affect this phenomena include the material properties of the encapsulant, chip size, substrate surface conditions, standoff height, dispensing pattern, etc. Given below is an equation that relates the flow velocity of the material to factors such as the surface tension, standoff height, wetting properties, viscosity, and flow distance [4].

Install Equation Editor and double-click here to view equation.

where:

$v_{\text{front}}$  is the velocity of the material flow front,

$\gamma$  is the encapsulant surface tension,  
 $h$  is the standoff height,  
 $\theta_1$  is the contact angle on the top surface,  
 $\theta_2$  is the contact angle on the bottom surface,  
 $\eta$  is the encapsulant viscosity,  
 $X$  is the flow distance at the time in question.

This expression needs to be corrected for the influence of substrate surface roughness and material aging (at room temperature and/or during actual flow). Besides, effective estimates of the scatter (or uncertainty) of the flow due to surface roughness, temperature control variations, aging and material variation are also important for the definition of a robust process.

To ensure that the flow can be completed before gelling occurs, the flow behavior of the underfill material needs to be well understood. Experiments have been performed to explore and understand the flow properties. These (discussed later in this paper) include the study of the temperature dependency of the encapsulant flow, an exploration of the effect of surface roughness, an investigation of the interaction between temperature and surface roughness and their combined effect on the velocity of encapsulant flow, and an examination of the effect of material aging. Also, the scatter of the encapsulant's flow behavior was characterized. The experimental procedure adopted, the data obtained, as well as the inferences made are introduced in the following sections. A model that can be used to determine optimal substrate preheat temperature is presented below. This model consists of two segments. The first segment determines the

temperature at which the encapsulant's flow is completed before gelling commences while the second segment considers the impact of variation in the material's flow and gelling time. It (the second segment) then predicts the probability that flow is completed before gelling begins.

### **3.0 DETERMINE THE TEMPERATURE AT WHICH THE FLOW IS COMPLETED WHEN GELLING BEGINS**

The substrate preheat temperature at which the underfilling of the chips has just been completed when gelling is initiated is application dependent. This temperature is the maximum feasible temperature at which a good underfill could be achieved. First, the time to complete the flow of the underfill material to a specific distance on a prototype specimen (smooth glass slides) was determined as a function of temperature. This was then corrected by factoring in the effect of the wetting characteristics and the surface roughness of the surfaces of the actual assembly. Finally, the effective optimal temperature needed to offer the tolerance required to cope with an aged material (material close to the end of its pot life) was estimated.

#### **3.1 Step One. Determine the Time Required to Complete Flow (To a Specific Distance) as a Function of Temperature**

The time required by the encapsulant to complete its flow during actual underfill of a chip was determined using a four stage approach. The stages are discussed below.

##### *3.1.1 Study the Temperature Dependency of Encapsulant Flow*

The flow of a fresh encapsulant sample was measured in between two smooth glass slides with a 0.076 mm

(3 mil) standoff at 70°C, 85°C, 100°C, 115°C, 130°C and 150°C. The time to flow to pre-defined distances was measured up to a maximum of twenty minutes or until the encapsulant stopped flowing (whichever occurred earlier). An encapsulant was said to have stopped flowing when it did not flow to the next increment of flow distance (1.59 mm or 1/16") within the next five minutes. Figure 1 shows the square of the flow distance versus the flow time for various substrate dispensing temperatures. The initial slope (S) exhibited a straight line (Figure 1) as expected [3]. The 'initial slope' is defined as the slope of the data collected when the flow distance is less than 20.64 mm (13/16"). A reasonably linear dependency was observed between the natural logarithmic value of the initial slope, S, of  $\dot{x}(t)$  and the reciprocal of temperature, as indicated below.

Install Equation Editor and double -  
click here to view equation.

These results agree well with an Arrhenius behavior of the viscosity [3].

The definition of the initial slope (S) as the slope of the data collected when the flow distance is less than 20.64 mm (13/16") seems to be subjective. The initial slope was therefore re-defined as the slope of the data whose  $R^2$  value is greater than 0.995 where the  $R^2$  value indicates the goodness of fit. Ascribing deviations from the straight line to material gelling, this re-definition of 'initial slope' also offers a definition of the onset of gelling. The logarithmic value of the initial slope was plotted versus the reciprocal of the temperature (Figure 2). An even better linear fit was observed (as indicated by the equation below).

Install Equation Editor and double -  
click here to view equation.

corresponding to an activation energy of 7.64 Kcal/mole for the viscosity [3].

The time,  $t_0$ , required to flow a distance,  $X$ , in a 3 mil gap between two glass slides now follows by inserting the slope

Install Equation Editor and double -  
click here to view equation.

Since

Install Equation Editor and double -  
click here to view equation.

and

Install Equation Editor and double -  
click here to view equation.

$t_0$  is given in seconds,  $X$  in mm, and the temperature  $T$  in degree Kelvin.

### *3.1.2 Correction for the Effects of Wetting*

The time to flow between a passivated chip surface and a solder mask surface is computed by correcting the time taken to flow between glass slides (Equation 2) for the effect of wetting. As the velocity of the flow front has a linear dependency on  $(\cos\theta_1 + \cos\theta_2)$  (Equation 1), the time to flow varies as the reciprocal of  $(\cos\theta_1 + \cos\theta_2)$ . The contact angles of the present encapsulant on a typical polyimide passivated chip surface and a solder mask surface were  $11^\circ$  and  $23^\circ$ , respectively. The contact angle on the glass slides was  $18^\circ$ .

### *3.1.3 Correction for the Effects of Surface Roughness*

First, a set of experiments were conducted to explore the effect of surface roughness. Smooth glass slides were frequently used in our experiments to simulate the capillary flow of the underfill material. The solder mask used in the actual assembly may, however, have a different degree of roughness. The impact of the surface roughness was found to depend on material properties such as the viscosity and particle sizes [3]. The effect of roughness is also known to depend on standoff height [4]. This segment of experiments helped to explore the effect of substrate surface texture on both the average flow rate and the scatter of the flow rate. The flow of fresh material was measured for three combinations of surface conditions, in between two smooth glass slides, between a smooth glass slide on the top and a frosted glass slide on the bottom, and between two frosted glass slides. The substrate preheat temperature used was 75°C and the standoff was 0.076 mm (3 mils). The experiments were duplicated six times to ensure the validity of the results and to explore the variation of the flow for each set of surfaces.

The data collected is plotted in Figure 3. The flow of the encapsulant was slower on rough surface(s). The average slopes of  $X^2$  versus  $t$  were found to be 64 mm<sup>2</sup>/min, 50 mm<sup>2</sup>/min and 36 mm<sup>2</sup>/min for the two smooth surfaces, the mixed case, and the two rough surfaces, respectively. With the two smooth surfaces as reference, one rough surface caused a decrease of 22% in the average slope and two rough surfaces a decrease of 42%.

The second set of experiments explored the interaction between temperature and surface roughness. The experiments described above were duplicated here at 100°C. The two surface conditions considered were

two smooth surfaces and a mixed set of surfaces (smooth surface on the top and frosted surface on the bottom). The flow of the encapsulant was again slower on rough surfaces. The average slope of  $X^2$  versus  $t$  was  $161 \text{ mm}^2/\text{min}$  between two smooth surfaces and 115 between the mixed surfaces, i.e. one rough surface caused a decrease of 29% in the average slope. This is quite similar to the reduction observed at  $75^\circ\text{C}$  (22%), but the scatter caused by surface roughness was more significant at the lower temperature. This will be further discussed later in this paper.

In a typical FCOB underfill process, the encapsulant is flowed in between the passivated chip surface and the solder mask surface. While the chip surface is relatively smooth, solder mask surfaces exhibit various degrees of roughness. Therefore, the flow in between a smooth surface and a rough surface may often best represent the flow in an actual assembly. The surface roughness of a solder mask surface may be different from the surface roughness of a frosted glass slide, but the effect of surface roughness on the encapsulant flow speed was found to be similar for different degrees of roughness, as long as the roughness is substantial [3]. This is believed to be because the filler particles in the encapsulant fill in the features of such a rough surface, so that the underfill material is actually flowing on a particle covered surface. Therefore, the effective surface roughness is only dependent on the particle size, shape and distribution.

In conclusion, the time to complete encapsulant flow to any distance between chip passivation and solder mask surfaces should usually be corrected to 129% of the value obtained on smooth surfaces.

### *3.1.4 Correction for the Effects of Material Aging*

The first set of experiments helped to study the effect of material aging (at room temperature) on the average encapsulant flow rate as well as on the flow rate variation. The flow of material was measured between two smooth glass slides with a 0.076 mm (3 mil) standoff height at 75°C for fifteen minutes. Materials under two aging conditions were considered; new material (stored for less than six hours at room temperature) and aged material (stored between twelve hours and sixteen hours at room temperature). While the effect of aging in the freezer was not included within the scope of this study, material used for this experiment had been stored in the freezer for less than three months. Previous research has indicated that a material that had been aged for a longer time had a greater tendency to form voids when flowed over longer distances [3]. Indeed, the location of voids and/or the time at which voiding begins was correlated to the deviation of the material's flow from its regular behavior (addressed later).

The flow of an aged material was slower than a non-aged material. The average slopes of  $X^2$  versus  $t$  were 64 mm<sup>2</sup>/min for a new material and 56 for an aged material, i.e. the aged material had an average slope which was 87% of that obtained for non-aged material. To ensure that the proposed process is feasible within the pot life of the entire material (which is given as sixteen hours by the manufacturer), the predicted flow behavior should thus be corrected for the material's aging effect. The time to complete flow was increased by 15% to account for this.

Install Equation Editor and double -  
click here to view equation.

The actual flow time,  $t_1$ , in a realistic assembly can be expressed as

where  $t_0$  is given by Equation (2) for the case of a 0.076 mm (3 mil) standoff, re-emphasizing that the roughness correction is also specific to this standoff. Therefore,

Install Equation Editor and double -  
click here to view equation.

$t_1$  thus indicates the time (in seconds) required to flow to a distance  $X$  (in mm) between a typical polyimide passivated chip surface and a solder mask surface for a 0.076 mm (3 mil) standoff height at a temperature  $T$  (in °K) if the underfill material is within the manufacturer's suggested pot life.

### **3.2 Step Two. Determine When Gelling Occurs**

As expected, the encapsulant flowed faster and gelled (stopped flowing) earlier when the temperature was higher (see Figure 1). The present encapsulant did not stop flowing within the duration of the experiment (20 minutes) when the substrate's preheat temperature was 85°C or lower. The maximum flow distance is shorter at a higher substrate preheat temperature due to the gelling of the material. The following inferences were made to generate a model that could predict the time at which encapsulant flow stops. The cessation of material flow indicates a viscosity change (or gelling), and the time required for the flow to stop ( $t_2$ ) should thus correlate to a rate of chemical reaction as represented by the following equation.

Install Equation Editor and double -  
click here to view equation.

where:

$K_{\text{rate}}$  is reaction rate,

$E_a$  is the activation energy,

T is the temperature (K), and

A and k are constants.

Therefore [Install Equation Editor and double-click here to view equation.](#)

or [Install Equation Editor and double-click here to view equation.](#)

The time at which the flow stops should thus vary exponentially with  $1/T$ . Figure 4 indeed exhibits an almost linear dependency between the natural logarithmic value of the time to stop flowing and the reciprocal of temperature (the  $R^2$  value is 0.996). This is especially true at high temperatures, because at relatively low temperatures the definition of the cessation of encapsulant flow (see above) may not indicate the actual cessation of flow. A linear regression of the data points collected between  $100^\circ\text{C}$  and  $150^\circ\text{C}$  indicates that

[Install Equation Editor and double-click here to view equation.](#)

corresponding to an activation energy  $E_a = 18.74$  Kcal/mole.

The time estimate for the completion of encapsulant flow was based on the initial slope of  $X^2$  versus t. If

the occurrence of gelling is defined as the cessation of material flow, the effect of the initial slowing down of the encapsulant flow needs to be considered. Also, previous experience indicates that for aged materials voiding occurs when the material flows over longer distances [3]. Therefore, it may not be appropriate to use the time at which encapsulant flow stops as a threshold value. To ensure a robust process, the threshold at which gelling is initiated was instead defined as the time that the flow of material deviates from normal behavior, i.e. when  $X^2$  versus  $t$  deviates from a straight line with a  $R^2$  value greater than 0.995. Figure 5 shows the natural logarithmic value of this gelling time versus the reciprocal of temperature. A linear dependency is still observed:

Install Equation Editor and double-click here to view equation.

which leads to

Install Equation Editor and double-click here to view equation.

corresponding to an activation energy  $E_a' = 16.64$  Kcal/mole for gelling. Here,  $t_2$  is the time required for the encapsulant to gel (deviate from its normal flow behavior) at a preheat temperature  $T$ .

### **3.3 Step Three. Determine the Maximum Temperature At Which Flow Is Completed When Gelling Begins**

At a higher temperature, encapsulant flow is completed faster and gelling begins earlier. However, the activation energy for the viscosity (7.64 Kcal/mole) is much smaller than that for 'gelling' (16.64 Kcal/mole), so that the time at which gelling begins decreases faster than the time required to complete flow.

Therefore, there exists a maximum temperature at which the flow can still be completed before gelling begins. At this temperature,

Install Equation Editor and double -  
click here to view equation.

or

Install Equation Editor and double -  
click here to view equation.

It follows that the maximum temperature at which flow can be completed before gelling begins is

Install Equation Editor and double -  
click here to view equation.

For a 12.7 mm x 12.7 mm (½" x ½") polyimide passivated chip with a 0.076 mm (3 mil) standoff height, the maximum substrate preheat temperature is therefore 127°C for the encapsulant studied if it is used within a 16 hour pot life. The time to complete flow will be 52.7 seconds. However, the substrate preheat temperature indicated here was determined without considering variation in the encapsulant flowtime or the time at which gelling begins. For symmetric distributions of both flow time and 'gelling' this means only a 50% 'yield'! Of course, the present definition of 'gelling' does not imply the cessation of flow, but it may indicate an onset of voiding (discussion provided in Section 5).

#### **4.0 PREDICT THE PROBABILITY THAT FLOW IS COMPLETED BEFORE GELLING BEGINS**

A robust underfill process needs to consider the variation in the material as well as the process environment.

Based on the understanding of the sources of the scatter and their effects, the probability that a good underfill will be obtained can be predicted. For a given probability criteria (6s), the maximum substrate preheat temperature which can be used can thus be determined.

#### **4.1 The Variation of the Time to Complete Flow**

The **first step** was to evaluate the factors that affect the scatter in the encapsulant's flow time. The scatter in the observed flow time may be caused by factors such as the surface roughness, material aging, material variation, temperature variation, etc. Figure 6 shows the individual slope (of six duplications) divided by the average slope for the different cases (with different surface texture, aging, and temperature). The standard deviation of the slope divided by the average slope (Std/Avg) was used to indicate the relative scatter in material flow time. A new material flowed in between two smooth glass slides at a substrate preheat temperature of 75°C resulted in the least scatter (3.3%). This was used as the reference condition. For a mixed set of surfaces, the scatter increased by a factor of almost two, to 6%.

A higher substrate preheat temperature (105°C) also resulted in more scatter (6.8%). However, in this case, a mixed set of surfaces did not cause additional scatter in the flow time. This suggests that the effect of a rough surface on the scatter of flow time is less significant at a higher temperature. Besides, the flow of an aged material also exhibited about twice the scatter as in the reference condition. The above mentioned effects on scatter are also visible in Figure 3. Therefore, the worst condition (most scatter) is the flow of an aged encapsulant on a rough surface (in a mixed set of surfaces) at a high temperature. The standard deviation of the  $X^2(t)$  slope divided by the average slope (Std/Avg) for an aged material flowing

between a rough and a smooth surface at high temperature was estimated by Equation 4. The Std/Avg for the case of a new material between smooth surfaces is denoted as  $s_{Std/Avg-0}$  and the scatter due to material aging as  $s_{Std/Avg-A}$ . The variance of the combined factors is then:

Install Equation Editor and double -  
click here to view equation.

Then at 75°C

Install Equation Editor and double -  
click here to view equation.

i.e.  $s_{Std/Avg-A} = 0.059$ .

If it is assumed that the scatter caused by material aging is independent of temperature, then the Std/Avg for the aged material flow on a rough surface at a substrate preheat temperature of 105°C can be estimated as:

Install Equation Editor and double -  
click here to view equation.

The **second step** was to evaluate the scatter of the flow time for specific flow distances. The scatter of the slope of  $X^2(t)$  was characterized in the previous (first) step. However, this does not include the effects of the scatter of individual flow times around the straight line fit to the corresponding  $X^2(t)$ . The present section intends to characterize the scatter observed in the actual time to flow to a specific distance. For all cases, more scatter was observed at a longer flow distance or over a longer flow time (Figure 3). Figure 7 shows the ratio of the time to flow to various flow distances to the average (time to flow) for the case in which

material flowed on smooth surfaces at 75°C. The initial values of this ratio exhibit significant variation. This may be due to the error in the initial measurement caused by manual dispensing of the encapsulant and the problems associated with collecting precise data when material flows fast through a shorter flow distance. This error was magnified when data was divided by the average flow time which is a small number. Other than that (the initial variation), the scatter observed in the ratio of the time to flow through various flow distances to the average (time to flow) for different cases seems to be independent of flow distance. This suggests that the scatter varies linearly with the average flow time.

To further quantify this, the ratios of variance and standard deviation to the average are plotted as functions of the flow distance. The ratio of variance in the flow time to the average flow time did not exhibit any systematic trend when plotted as a function of flow distance. However, the ratio of the standard deviation in the flow time to the average flow time appears reasonably constant for most cases (Figure 8). This indicates that the standard deviation of the time to flow to any distance is proportional to the average flow time for all cases. The following equation was used to denote that the random variable “X” is normally distributed with a mean value of  $\mu$  and a standard deviation of  $s$ .

Install Equation Editor and double -  
click here to view equation.

The time to complete flow then follows as:

Install Equation Editor and double -  
click here to view equation.

For each case (with different surface texture, aging, and temperature), the value of  $s_0$  can be determined

by averaging the values of the ratio of the standard deviation of the flow time to the average flow time for different flow distances. The initial data points (which were assumed to be erroneous as discussed above) were not included in calculating the value of  $s_0$  (Figures 8). The  $s_0$  for the flow of an aged material on a mixed surface at 100°C was estimated as 0.1049 (using Equation 4). As mentioned above, this is larger than the 8.9% scatter in the slopes because of the scatter within the individual  $X^2(t)$ -sets. As the expected value of  $t_1 = X^2/S$  was determined in the previous section, the standard deviation can be expressed as a

Install Equation Editor and double -  
click here to view equation.

function of temperature and distance to flow, and

#### **4.2 The Variation of Material Gel Time**

The flow of new material in between two smooth glass slides with a 0.076 mm (3 mil) standoff height was measured at 100°C. This experiment was duplicated six times to obtain the variation (standard deviation) in the time needed for the material to begin gelling (deviating from an expected flow behavior with a  $R^2$  value of less than 0.995). While the variation of the time required for gelling to begin may be temperature dependent, it was not considered as such in this research. The average time to gel was 5.67 minutes with a standard deviation of 0.74. Therefore, the time for the gelling to begin can be expressed as

Install Equation Editor and double -  
click here to view equation.

### 4.3 Probability That Flow Is Completed Before Gelling Begins

The time required to complete encapsulant flow,  $T_1$ , and the time at which gelling begins,  $T_2$ , are considered as two random variables with known distributions.

$$T_1 = N(t_1; \mu_1, s_1)$$

$$T_2 = N(t_2; \mu_2, s_2)$$

Install Equation Editor and double -  
click here to view equation.

Install Equation Editor and double -  
click here to view equation.

If  $T_1$  and  $T_2$  are assumed to be two independent normal distributions, then

Install Equation Editor and double -  
click here to view equation.

Since the difference of two normally distributed random variables can be expressed as

it follows that

Install Equation Editor and double-click here to view equation.

where  $F$  is the cumulative distribution of a standard normal random variable, with a mean value of zero and a standard deviation of one [5].

In the case of a 12.7mm square chip with a 0.076 mm (3 mil) standoff from the solder mask surface and preheated to a temperature of 100°C, the probability that flow can be completed before gelling is initiated is thus 0.9981. For a preheat temperature of 94.5°C, on the other hand, the probability of defective underfilling would be as low as 2.4 ppm, and the criteria of six sigma would be satisfied.

## **5.0 CORRELATION BETWEEN VOIDING AND GELLING**

During the underfill experiments that were conducted to observe the variation in the time needed for the underfill material to gel, the formation of voids was also observed and recorded. The voids were always located at larger flow distances, within areas which appeared lighter during optical inspection (Figure 9).

This scenario correlated to the patterns found in previous assemblies [3] as the darker area in the gray scale images generated by the Scanning Acoustic Microscope (SAM). Factors that could cause this scenario included differences in filler concentration (or orientation), concentration of coloring agents, interior voids and porosity in the material. The time and the location of the first voids as well as the location where the lighter pattern begins were compared to the data point at which  $X^2(t)$  deviates from a straight line (Figure

10). It is seen that voiding is initiated even before the material flow begins to deviate from a straight line with a  $R^2$  of 0.995. In other words, voiding can be seen before gelling begins.

## **6.0 CONCLUSION**

The global objective of this study was to develop a model to predict the optimal substrate preheat temperature for use in the underfill process. This optimal temperature should depend on factors such as the underfill material used, the size of the chip, the surface condition, the bump layout, the standoff height, etc.

Some of the defects that can be induced by the adoption of high preheat temperatures were evaluated.

The preheat temperatures used in this study did not impact filler settling, and the size and number of voids.

Other possible consequences such as the impact on interface adhesion should be explored. The completion of capillary flow before the gelling begins is a primary concern when higher preheat temperatures are used. Experiments were done to understand the flow behavior and gelling of the underfill material.

While the optimal temperature determined by the initial version of the model was the temperature at which the flow was completed just when the gelling of the material began, the second part considered the scatter in the flow time and in the time at which gelling began. Assuming independent, normal distributions of flow times a six sigma criterion was used to evaluate the feasibility of any given substrate preheat temperature.

The optimal temperature for substrate preheat was inferred.

A specific encapsulant was chosen for this study. For now, reproducibility studies were limited to variations within a single batch of this encapsulant, although aging effects were considered. When the prediction

model did not consider scatter in data, the results obtained suggested 127°C and 182.5°C as the optimal temperatures for chip sizes of 12.7 mm (½") and 6.35 mm (¼") square, respectively (Table 1). These temperatures are in contrast to the substrate preheat temperature of 70°C suggested by the manufacturer.

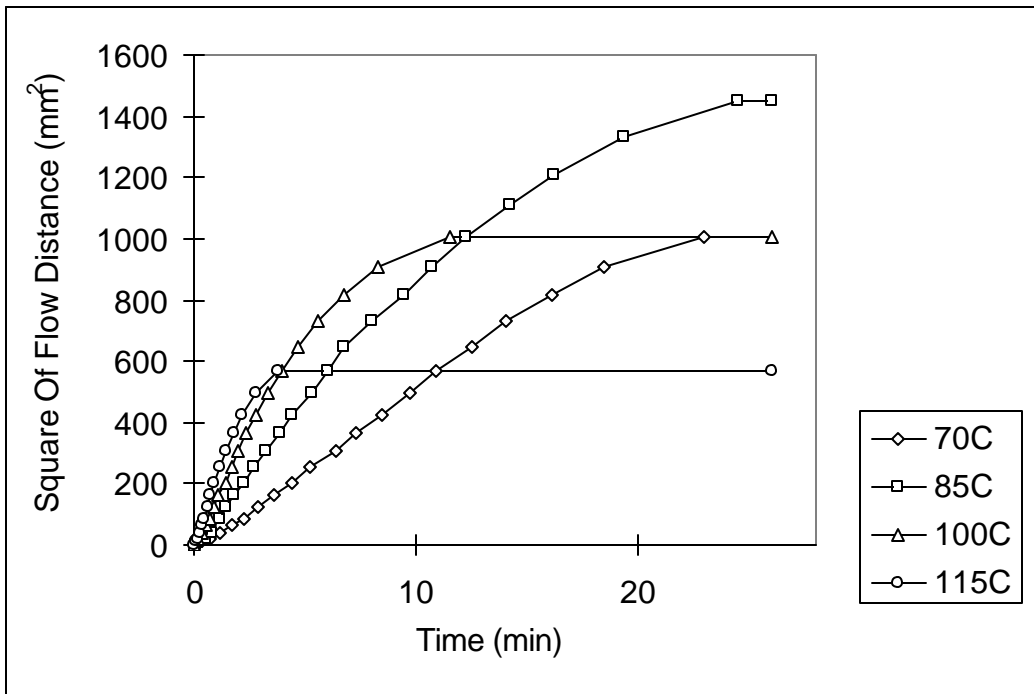
If the substrate preheat temperatures recommended without considering scatter in the data are used, the encapsulant's flow time can be reduced from 4.36 minutes to 0.88 minutes for the 12.7 mm (½") square chip and from 1.09 to 0.07 for the 6.35 mm (¼") square chip. When the scatter in the flow times and the gel times are considered, the suggested optimal substrate preheat temperatures are 94.5°C and 100°C, respectively. The time for the flow to complete can then be reduced from 4.36 minutes to 1.77 minutes and from 1.09 minutes to 0.44 minutes, respectively. A 60% reduction in the process time can thus be achieved. It is expected that this reduction in process time varies strongly with materials (especially for some snap cure materials). The proposed model could be enhanced by considering other factors such as the impact of flux residues, interface adhesion, etc.

## REFERENCES

- [1] Coombs, C.F., 'Printed Circuits Handbook', Fourth Edition, McGraw Hill, New York, 1995.
- [2] Giesler, J., O'Malley, G., Williams, M, & Machuga, S., 'Flip Chip On Board Connection Technology: Process Characterization And Reliability', IEEE Transactions on Components, Packaging, And Manufacturing Technology, Vol.17, No.3, 1994, pp. 256-63.
- [3] Huang, C-Y, 'Process Research in the Encapsulation of Direct Chip Attach Components', Doctoral Dissertation, State University of New York, Binghamton, New York, May 1996.
- [4] Fosberry, J, 'An Investigation of The Physical Properties And flow Behaviors of Encapsulant Materials for Direct Chip Attach Applications', Masters Thesis, State University of New York, Binghamton, New York, August 1996.
- [5] Devore, J. L., 'Probability and Statistics for Engineering and the Sciences', Brooks/Cole Publishing

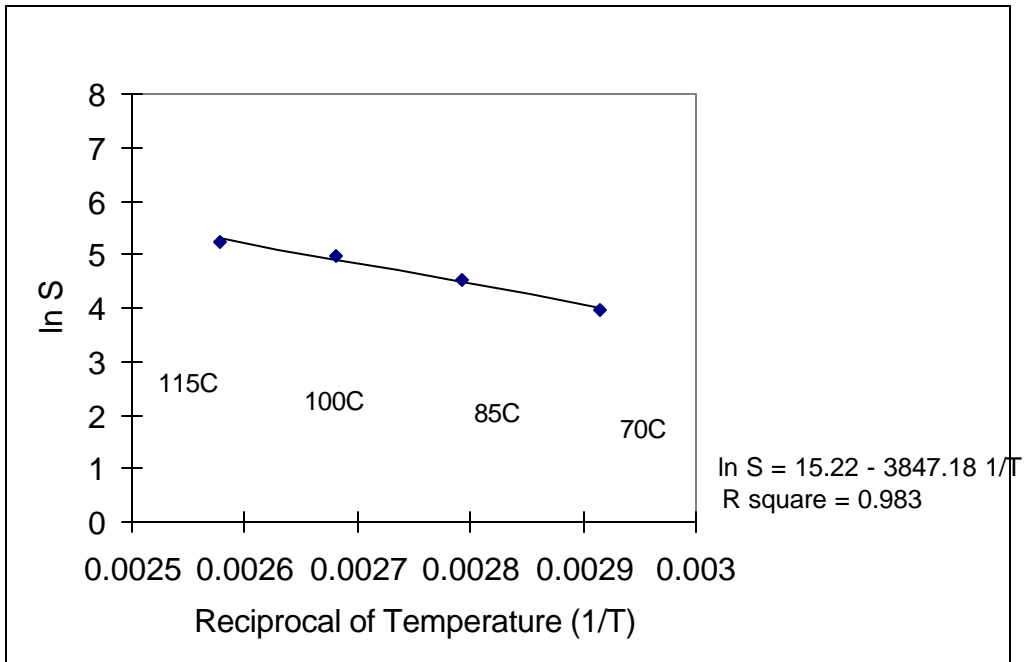
Company, Pacific Grove, California, 1990.

Figure 1.



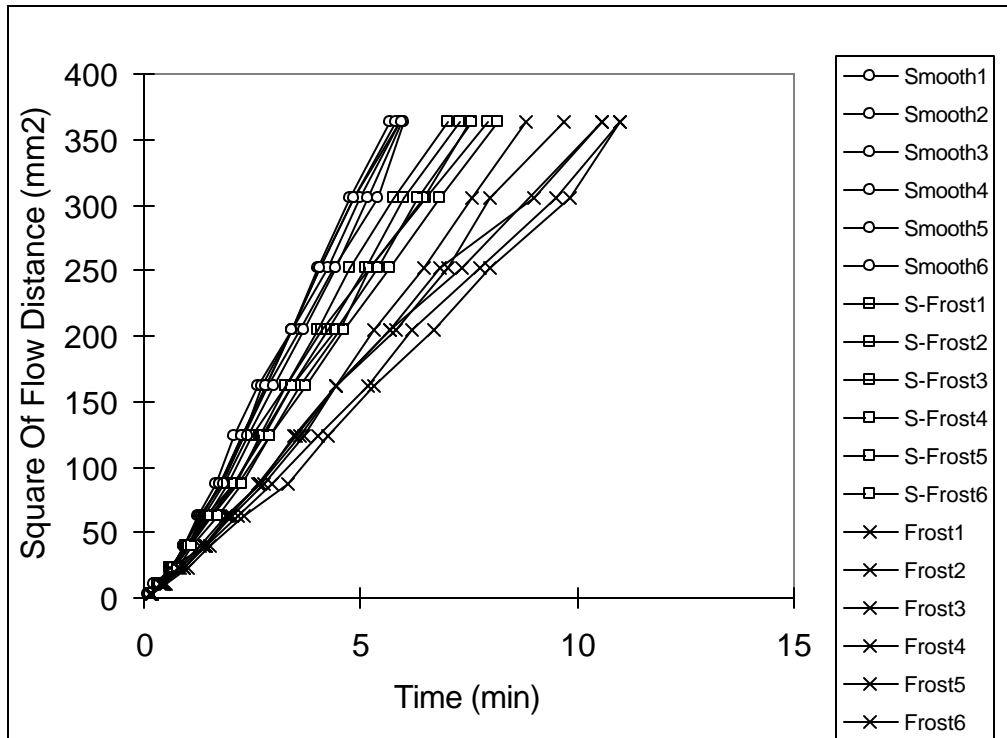
The Square of Flow Distance Versus Flow Time for Various Substrate Preheat Temperatures

Figure 2.



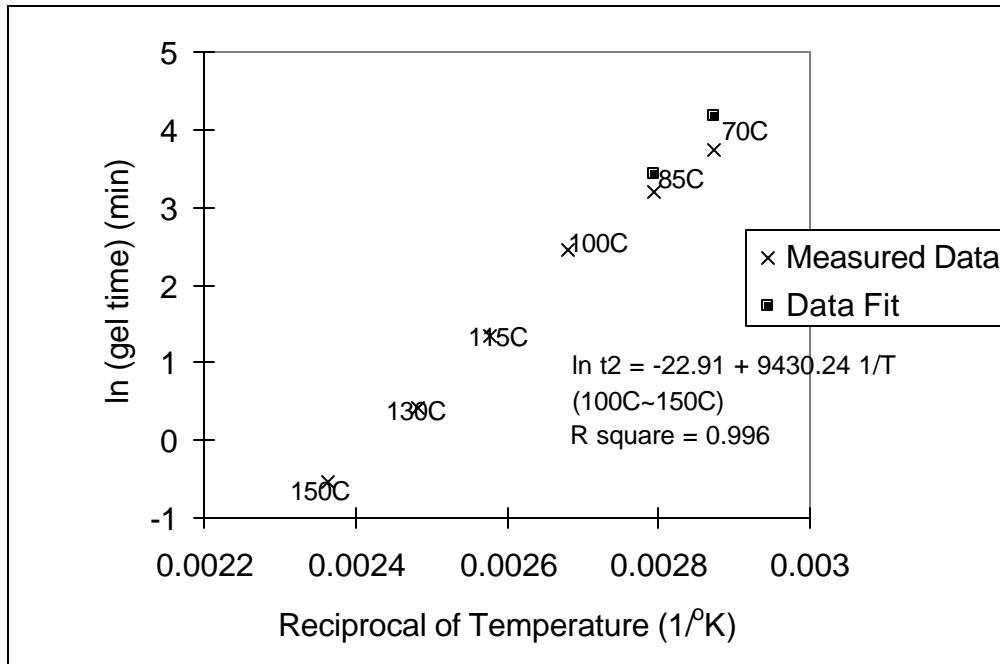
Initial Slope of  $X_2(t)$  Versus the Reciprocal of Temperature (When the Initial Slope Is Defined as the Slope of the Data That Does Not Deviate from a Straight Line)

Figure 3.



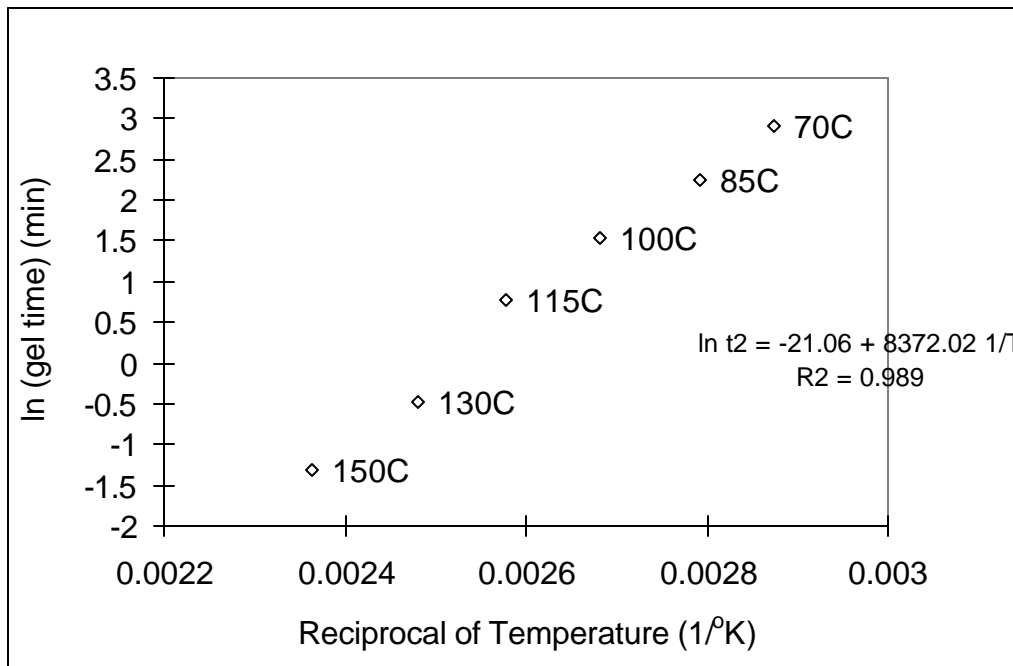
The Square of the Flow Distance Versus the Flow Time on Different Surface Roughnesses with a Substrate Preheat Temperature of 75oC

Figure 4.



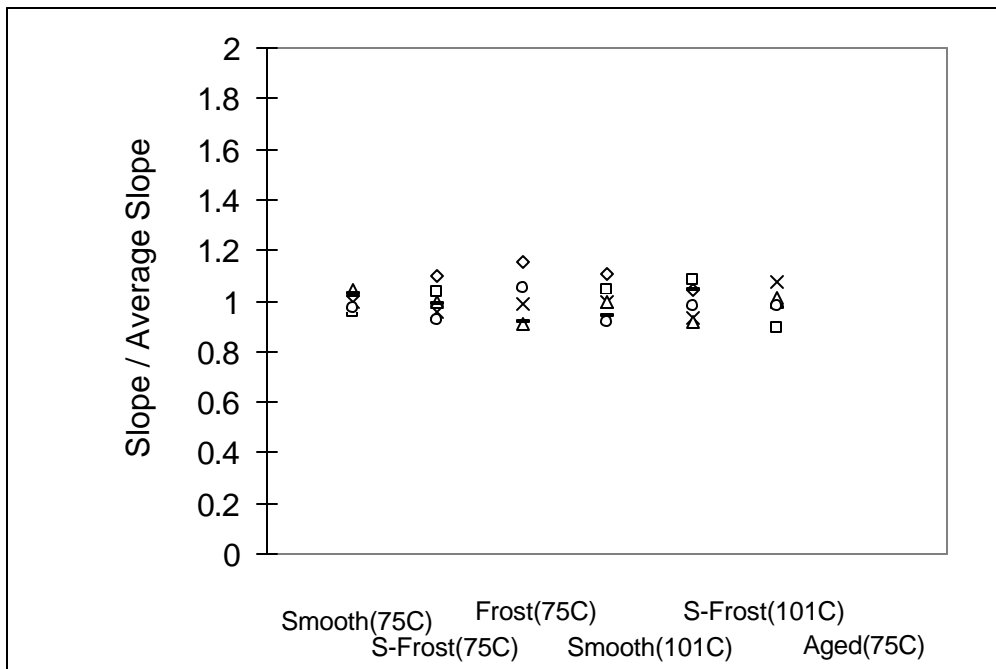
The Time to Gel Versus the Reciprocal of Temperature When the Gelling Is Defined as the Cessation of Material Flow

Figure 5.



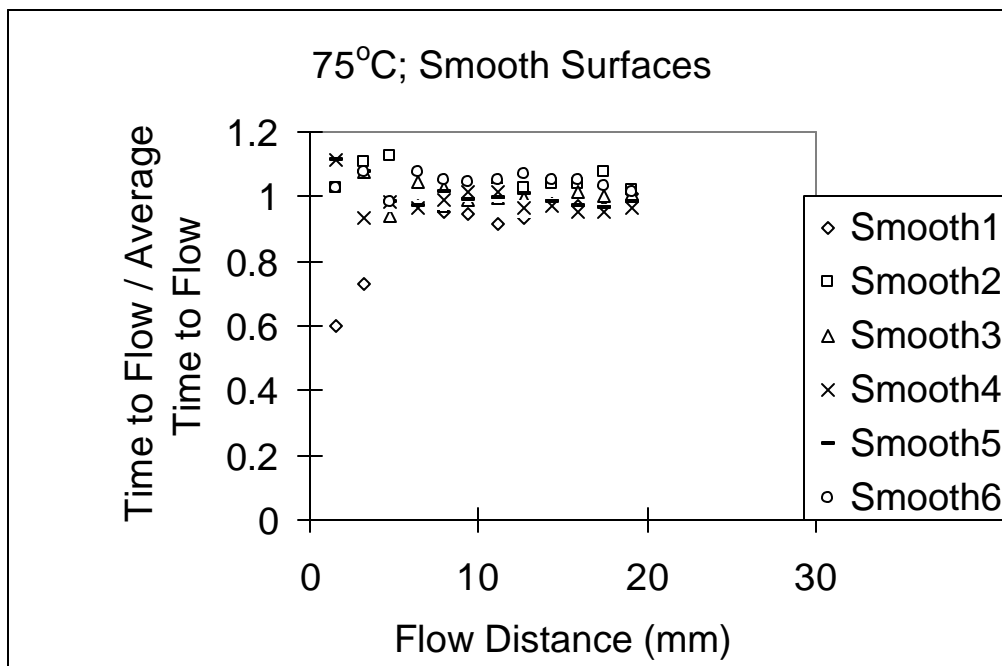
The Time to Gel Versus the Reciprocal of Temperature When the Gelling Is Defined as the Deviation of Flow From Normal Behavior

Figure 6.



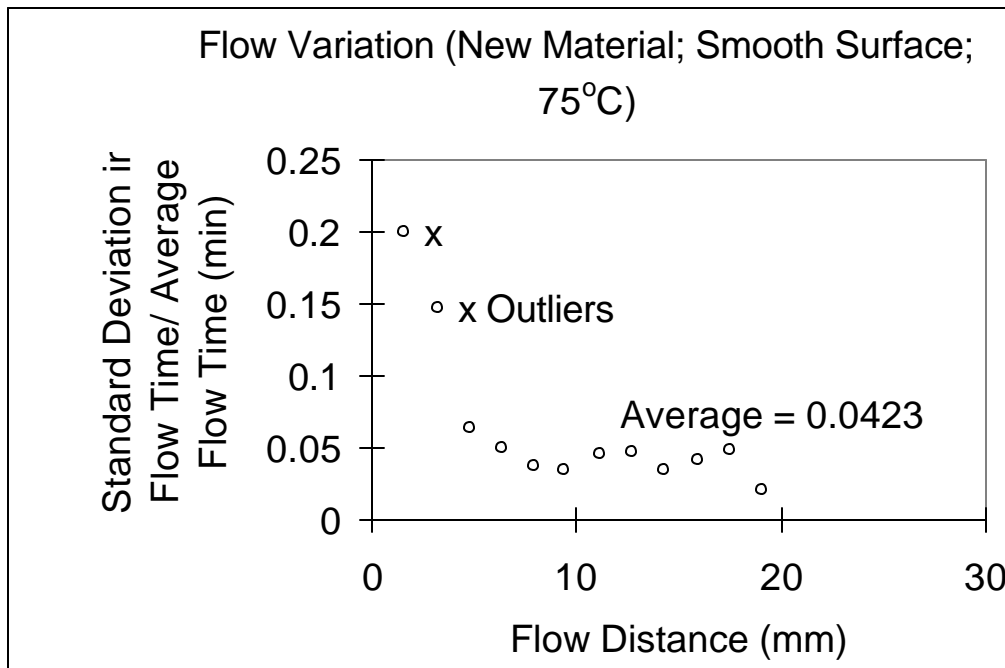
The Individual Slope of  $X_2(t)$  of Six Duplications Divided by the Average Slope For Different Cases (Surface Texture, Aging, and Temperature)

Figure 7.



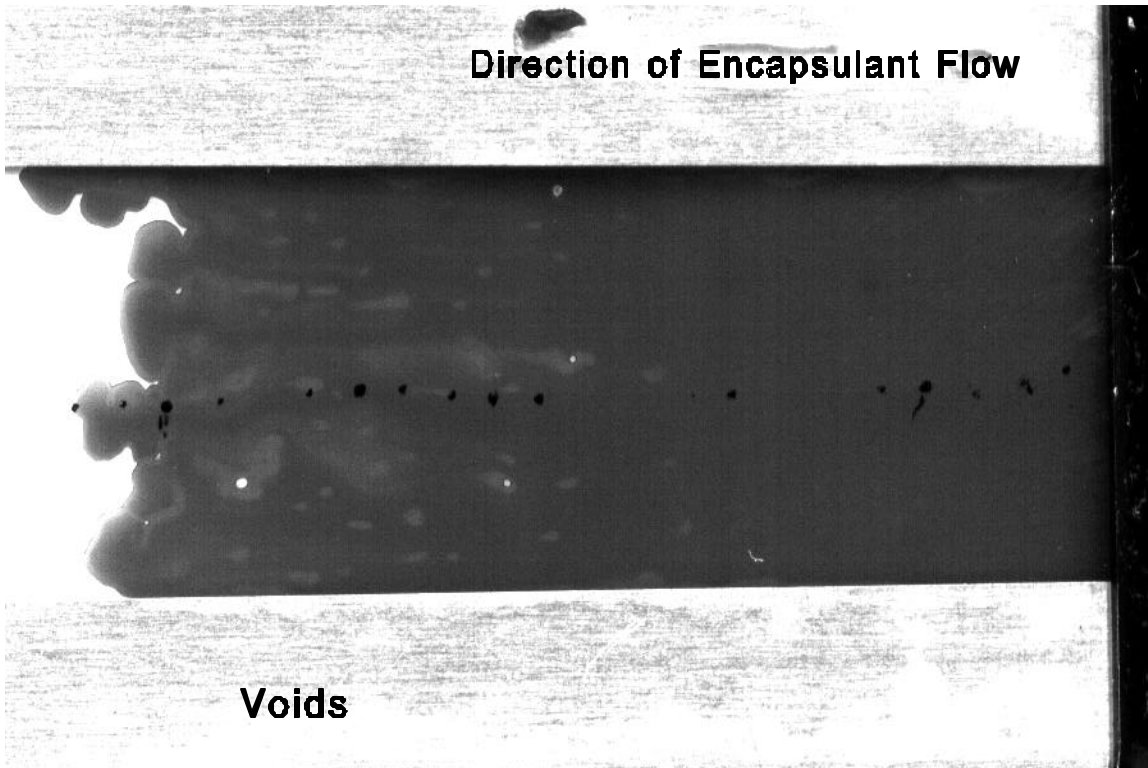
The Ratio of the Flow Time for Various Flow Distances to the Average (Time to Flow) for Different Cases (Surface Texture, Aging, and Temperature)

Figure 8.



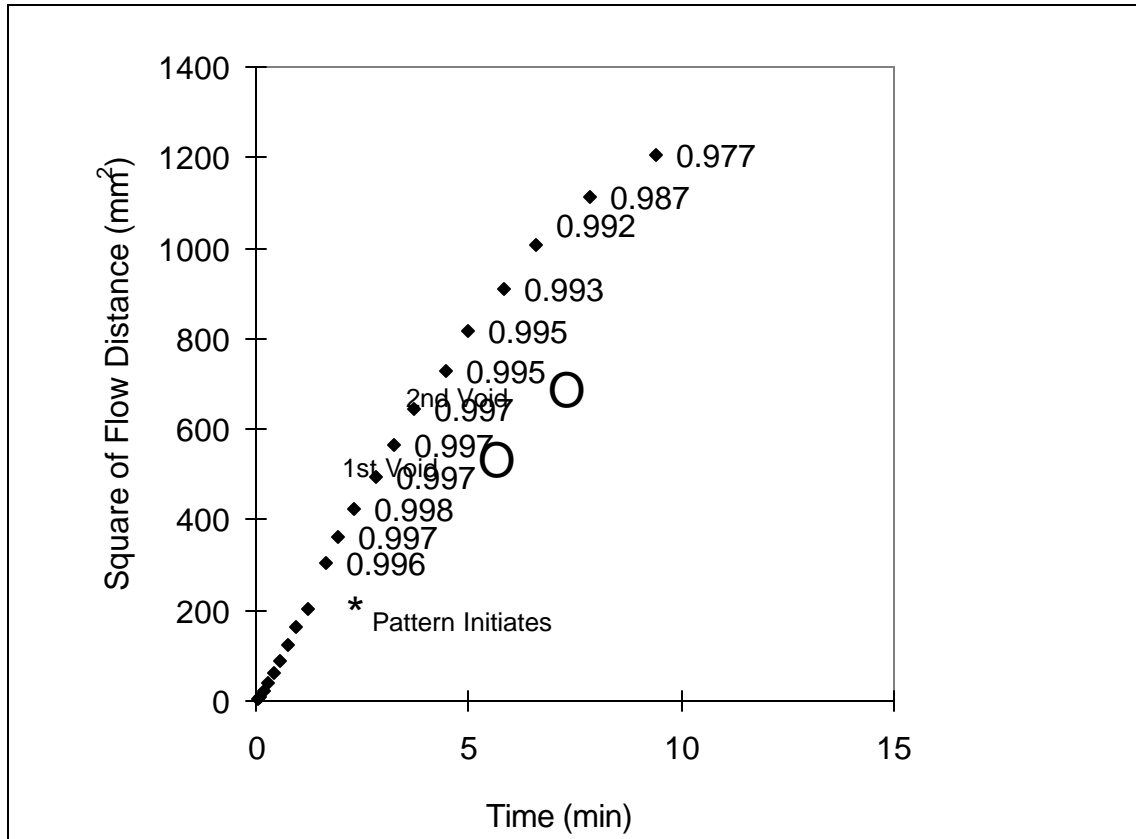
The Ratio of the Standard Deviation of the Flow Time to the Average Flow Time as a Function of Flow Distance

Figure 9.



A Sample of the Model Experiments Which Shows the Typical Locations of Voids

Figure 10.



The Time and Location of Voids and the Data Point at Which the Slope of  $X^2$  Versus  $T$  Deviates from a Straight Line

Table 1.

**Flow Times & “Gel” Times Vs. Temperature and Resulting Defect Levels  
for Two Chip Sizes**

(0.003 inches Standoff Height; Polyimide Passivated Chip & Typical Solder Mask Surface)

<b>Chip Size (Length in inch)</b>	<b>0.5</b>	<b>0.5</b>	<b>0.5</b>	<b>0.25</b>	<b>0.25</b>	<b>0.25</b>
<b>(Length in mm)</b>	12.7	12.7	12.7	6.35	6.35	6.35
<b>Substrate Preheat Temperature (C)</b>	<b>127</b>	<b>94.5</b>	<b>70</b>	<b>182.5</b>	<b>100</b>	<b>70</b>
<b>Time to Complete Flow (t1) (min)</b>	<b>0.88</b>	<b>2.07</b>	<b>4.36</b>	<b>0.07</b>	<b>0.44</b>	<b>1.09</b>
<b>(sec)</b>	53.0	124.0	261.8	4.1	26.6	65.5
<b>Time to Initiate Gelling (t2) (min)</b>	0.88	5.59	28.45	0.07	4.00	28.45
<b>(sec)</b>	52.7	335.4	1707.1	4.1	239.7	1707.1
<b>Flow Time Standard Deviation</b>	0.09	0.22	0.46	0.01	0.05	0.11
<b>Gel Time Standard Deviation</b>	0.74	0.74	0.74	0.74	0.74	0.74
<b>Standard Normal Random Variable (Z)</b>	0.01	-4.57	-27.68	0.00	-4.79	-36.54
<b>Probability That T1 &lt; T2</b>	0.497618	0.999998	1.000000	0.500106	0.999999	1.000000
<b>Defect Level (T1 &gt; T2)</b>	0.502382	<b>2.44E-06</b>	0	0.499894	<b>8.2943E-07</b>	0

Data Used to Illustrate the Results of the Preheat Temperature Optimization Model

